BOREAS An international journal of Quaternary research

Middle and Late Holocene relative sea level changes and coastal development at Rugård, Denmark

MARIE HOLST RIIS, LASSE SANDER, LARS NIELSEN, JAN-PIETER BUYLAERT, AMÉLIE JULIETTE MARIE CHALLIER AND NICOLAJ KROG LARSEN

BOREAS

Riis, M. H., Sander, L., Nielsen, L., Buylaert, J.-P., Challier, A. J. M. & Larsen, N. K. 2024 (January): Middle and Late Holocene relative sea level changes and coastal development at Rugård, Denmark. *Boreas*, Vol. 53, pp. 56–70. https://doi.org/10.1111/bor.12642. ISSN 0300-9483.

Denmark has been subject to complex interactions of isostatic uplift and eustatic sea level changes since the last deglaciation. Prominent coastal beach ridges as well as lagoonal and lake deposits from this period have been investigated at a number of sites in the region to constrain the relative sea level (RSL) changes. However, despite the common occurrence of former coastal lagoons and lakes in proximity to raised beach ridges, they have rarely been studied in combination. In this study, we use a multiproxy approach including geospatial data, lake sediment coring, ground penetrating radar and optically stimulated luminescence dating to investigate the Holocene coastal evolution and RSL history at Rugård in Mols Bjerge National Park, on the east coast of the Jutland Peninsula. Our results show that the coastal area at Rugård was transgressed between *c.* 7.6 and 7.0 cal. ka BP and that RSL was ~4.5 m higher than present between *c.* 6.6 and 5.9 ka ago, when the highest section of the beach ridge plain was deposited. The elevation and timing of this relative highstand are in good agreement with previous estimates of the Littorina transgression and contribute to our combined knowledge about RSL history and coastal evolution in the southern Kattegat. Subsequently, isostatic adjustment has caused uplift and erosion of the beach ridge plain, but renewed progradation and deposition of a lower beach plain have taken place since *c.* 1740 CE. Our results demonstrate the value of using a multiproxy approach to study RSL changes and coastal evolution.

Marie Holst Riis and Nicolaj Krog Larsen, Globe Institute, University of Copenhagen, Øster Voldgade 5-7, 1350 Copenhagen K, Denmark; Lasse Sander (corresponding author: lasse.sander@awi.de), Alfred-Wegener-Institute, Helmholtz Center for Polar and Marine Research, Hafenstraße 43, 25992 List/Sylt, Germany; Lars Nielsen, Geological Survey of Greenland and Denmark (GEUS), Øster Voldgade 10, 1350 Copenhagen K, Denmark; Jan-Pieter Buylaert and Amélie Juliette Marie Challier, Department of Physics, Technical University of Denmark, DTU Risø Campus, DK-4000 Roskilde, Denmark; *received 7th August 2023, accepted 1st November 2023.*

Mols Bjerge National Park, located on the east coast of the Jutland Peninsula, Denmark, was established in 2009 for its distinctive combination of both natural and cultural landscape types, and its value as a heritage site. The area is recognized for its glacial landscapes comprising large terminal moraines, dead-ice landscapes and outwash plains (Harder 1908; Pedersen & Petersen 1997). The glacial landforms were formed by ice lobes moving from a southeasterly direction during the Young Baltic Advance *c.* 19–18 ka ago (Houmark-Nielsen & Kjær 2003; Larsen *et al.* 2009; Houmark-Nielsen 2011). After the Last Glacial Maximum, sea level development was first dominated by the eustatic contributions of melting ice sheets, but was later locally outpaced by glacial isostatic uplift resulting in a relative sea level (RSL) fall in most of Denmark. The period of transgression, locally referred to as the Littorina transgression, left prominent coastal landforms at elevations of up to 13 m a.s.l. (metres above sea level) in northern Denmark and ~5.6 m a.s.l. within Mols Bjerge National Park (Mertz 1924). During the Middle- to Late Holocene, a diversity of coastal landforms developed in Denmark, comprising both erosive features, like cliffs and headlands, and depositional landforms, such as beach deposits, beach ridges, spits and coastal lagoons.

In southern Kattegat, several studies have addressed the origin and interpretation of raised postglacial marine landforms and sedimentary deposits, especially with regard to understanding RSL changes. These changes have mostly been reconstructed from accreted sedimentary deposits, such as lake or marine sediment cores (Christensen 1982; Hede 2003; Bennike *et al.* 2019, 2021) or from prograded coastal deposits, such as beach ridges or spits (Tanner 1993; Nielsen & Clemmensen 2009; Clemmensen *et al.* 2012; Hansen *et al.* 2012; Hede *et al.* 2015; Sander *et al.* 2016). These records show a fairly rapid Early Holocene RSL rise culminating in peak sea level *c.* 8–7 ka ago in northern Denmark and *c.* 6 ka ago further south around Mols Bjerge National Park (Christensen & Nielsen 2008). Although much is known about the general traits of Holocene coastal evolution and sea level history in Denmark, little is known about it within eastern Jutland.

In this study, we investigate landscape evolution and RSL history of the Rugård area in Mols Bjerge National Park using a combination of (i) geomorphological analysis of coastal landscape features, (ii) analysis of a sediment core from Teglkær Mose (bog), (iii) ground-penetrating radar (GPR) measurements across the beach ridge plain, and (iv) optically stimulated luminescence

DOI 10.1111/bor.12642

(OSL) dating of beach ridge deposits. Furthermore, we discuss the landscape evolution and Holocene RSL history in relation to other local and regional records from central Denmark.

Study area

The area of investigation is situated in a microtidal environment in the Kattegat region on the east coast of Jutland, Denmark (Fig. 1). The coastal section of Rugård is located within an almost 40-km-long stretch of shoreline facing the southern Kattegat. The area is mainly exposed to waves from the southern and eastern sector with a maximum fetch of up to 120 km. The shoreline is located at the transition between a glacial landscape, formed by the Main Weichselian Advance from a northeastern direction reaching its maximum position at the Main Stationary Line *c*. 23–21 ka ago, and a large terminal moraine system formed during the Young Baltic Advance that reached the area from a south-eastern direction *c*. 19–18 ka ago (Houmark-Nielsen & Kjær 2003; Larsen *et al*. 2009; Houmark-Nielsen 2011).

The research area at Rugård is situated in a topographic depression delimited by two headlands, with elevations of 25–50 m a.s.l., that are composed of unconsolidated glacial and proglacial meltwater deposits in the north and clayey till in the south (Pedersen

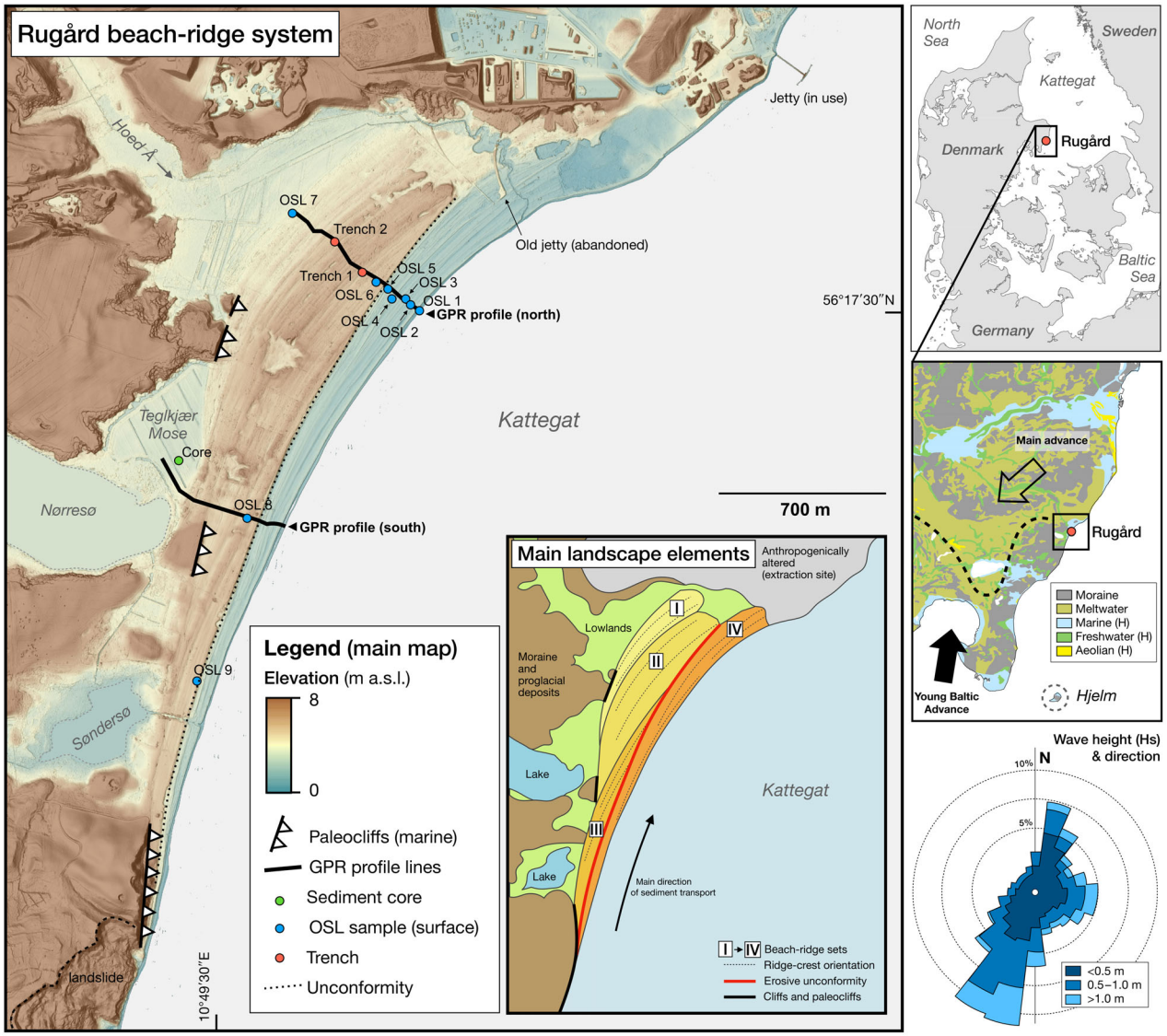

Fig. 1. Overview map of the research area at Rugård, Danmark. The main map (left) shows the topography and the locations of all sampling sites and an explanatory map of the main landscape features referred to in the text. The map panel on the right shows an overview map of the area (top) and a detailed map indicating the age (H = Holocene) and origin of Quaternary surface deposits in eastern Djursland (modified from GEUS 2023). The wave rose in the lower right corner indicates the significant wave height and direction of waves approaching the coast of eastern Djursland (modified from Danish Coastal Authority 2010).

& Petersen 1997). The coastal deposits primarily consist of marine sands and gravels that were deposited in a succession of beach ridges and that are now partly covered by aeolian sand (Pedersen & Petersen 1997). In the southern part of the research area, the formation of these beach ridges led to the isolation of coastal lakes and bogs, which has resulted in local formation of peat and other freshwater deposits. Along their landward boundary, these near-coastal wetlands are topographically confined by the tills. A small creek (Hoed Å), which was part of the proglacial drainage system, enters the coastal waters north of the beach ridge system. Across the creek, limestone from the Danien lies close to the surface below the glacial deposits (Larsen & Knudsen 1983) and an extraction site is located here. For shipping of the limestone, a road and jetty connected the extraction site with the deeper water offshore.

Material and methods

Geospatial data

In order to better describe and constrain the processes behind the past evolution of the coastal environment at Rugård, a suite of readily available geospatial datasets (Table 1) was employed to obtain information on the topography, bathymetry and composition of the surface deposits. In addition, a georeferenced series of historical maps roughly covering the time period since the late 18th century has been used with the aim of better understanding historical shoreline changes. All data were analysed in a geographic information system and information on the main data properties, sources and references are provided in Table 1.

Table 1. Maps used in this study. 1 = Dataforsyningen (2023); 2 = GEUS (2023); 3 = Danish Geodata Agency (2023); 4 = Contour lines from 1877 CE.

Map type/ collection	Year of measurement	Year of publication (CE)	Scale	Reference
DEM: DHM/ Terræn		2016		1
Geological surface map, v. 6.0		2021	1:25 000	2
Parish map	1780	1811	1:4000	3
Høje målebordsblade	1877	1878	1:20 000	1
Lave målebordsblade	1877, edited 1900	1903–1904	1:20 000	1
4 cm map	1875–1877, drawn and edited 1971–1974	1974–1975	1:25 000	1
4 cm map	1984–1985	1988	1:25 000	1, 4
DTK/Kort 50		2002	1:50 000	1
DTK/Kort 50		2011	1:50 000	1
DTK/Kort 50		2015	1:50 000	1
DTK/Kort 50		2017	1:50 000	1

Sediment core

A Russian peat corer was used to obtain a composite sediment core with a length of 274 cm from Teglkær Mose (bog) (56.2861°N, 10.8222°E; 3.1 m a.s.l.; Fig. 2). The bog itself has been drained since at least 1811 CE (Parish map). After the core was retrieved, it was sealed in plastic and stored at 4 °C. The position of the core was recorded with a handheld Garmin GPSMAP 64S (horizontal accuracy ±3 m) and the surface elevation of the bog was later obtained from the LiDAR digital elevation model (DEM) with an assigned vertical accuracy of ±0.05 m.

The core was cleaned in the laboratory and scanned using an ITRAX µXRF scanner at Globe Institute, University of Copenhagen, Denmark. The 1-m core sections were photographed, X-ray scanned, and X-ray fluorescence (XRF) measurements were made with a rhodium tube at intervals of 1 mm and with an exposure time of 30 s. Before the XRF scan, the core was covered with 1.4 µm Mylar® film to avoid water vapour between the core and the scanner. Ca/Fe and Sr/Ca ratios were used to identify transitions from marine to freshwater environment, and Ti/(inc + coh) ratios were used to identify transitions between organic-rich gyttja and more clastic sandy/clayey silt layers (Croudace & Rothwell 2015; Strunk *et al.* 2018).

The age of the sediment was determined using radiocarbon (^{14}C) dating of terrestrial macrofossils or marine shells. A single bulk peat sample was dated in one interval where it was impossible to find macrofossils; this is not normally recommended because of the risk of contamination with old carbon (Olsen *et al.* 2012). Accelerator mass spectrometry measurements were conducted at the Tandem Laboratory, Uppsala University, Sweden. The ^{14}C ages were calibrated to calendar years using rBacon version 3.0.0 (Blaauw & Christen 2011) with the calibration curves IntCal20 (Reimer *et al.* 2020) and Marine20 (Heaton *et al.* 2020). For the marine samples, we use a regional ΔR value of −141±119 years, based on the five nearest locations in the Marine20 database excluding samples from Limfjorden and Randers Fjord (Olsson 1980; Heier-Nielsen *et al.* 1995). A similar ΔR value is used by Bennike *et al.* (2021).

Georadar

Several studies on coastal environments use GPR as a method to chart the internal structure of beach ridge deposits and to estimate past RSL (Hein *et al.* 2013; Fruergaard *et al.* 2015; Hede *et al.* 2015; Van Heteren *et al.* 1998). The transition between the sloping beachface and the flatter upper shoreface is used as an indication of past sea level position (Tamura *et al.* 2008; Hede *et al.* 2015; Figueiredo & Rockwell 2022). For the microtidal context of the Kattegat Sea, Nielsen & Clemmensen (2009) and Hede *et al.* (2013) show that the

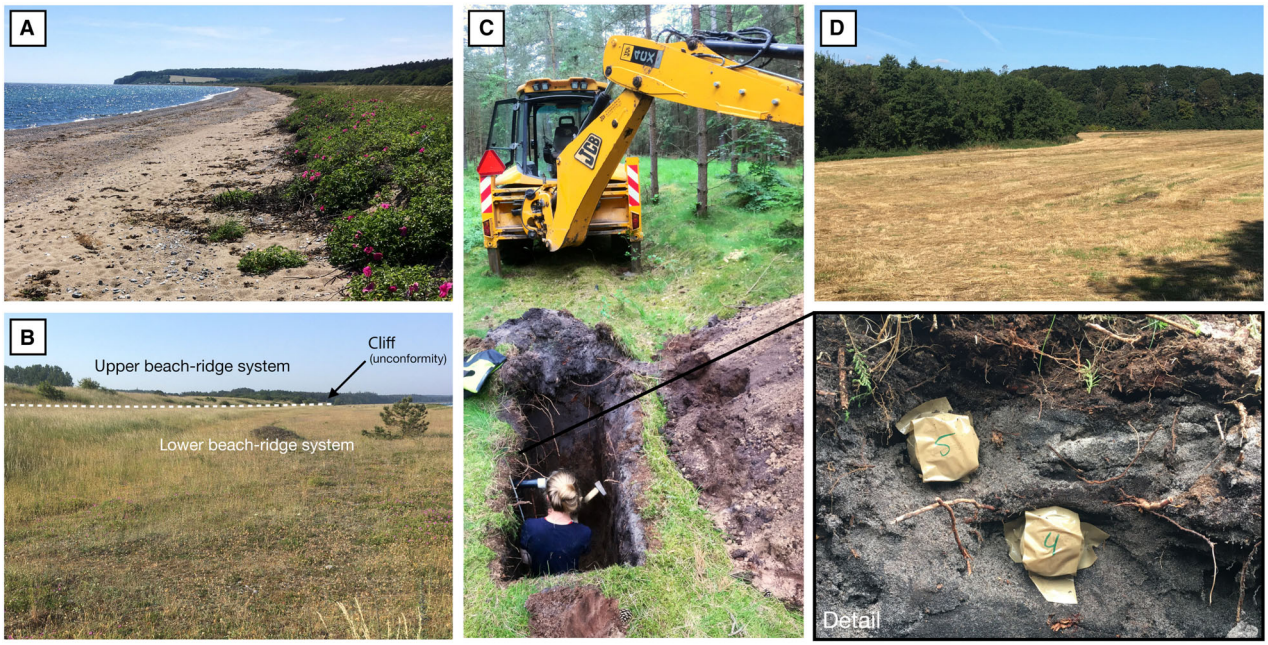

Fig. 2. Field pictures. A. Modern beach. B. The cliff that marks the transition between the upper (set III) and lower parts (set IV) of the beach ridge system (cf. Fig. 1). C. Trench and sampling from aeolian deposits of the upper beach ridge system. D. Flat surface topography of the former bog at Teglkær Mose.

elevation of the transition in the beach profile corresponds well with the mean sea level. In this study, points are marked in the data at positions where steeper reflections meet less steep reflections, in the form of either a downlap or a change in slope. Sea level estimates at the time of deposition are based on the general elevation of these points over distances of ~50–100 m, and the vertical accuracy of past sea level is estimated to ±0.5 m. This uncertainty accounts for limits in the vertical resolution of the GPR data, uncertainties in the velocity model used for migration and depth conversion as well as the uncertainties of the topographic data (see below). The ages of the deposits are estimated based on OSL dates on material from the beach ridges (see below).

Two transects perpendicular to the crest orientation of the beach ridges were recorded using GPR (Fig. 1). The northern transect starts from a back-barrier environment at the edge of the modern plantation in the NW and runs along a path towards the coast in the SE and is divided into four profiles (LINE66-69). The southern transect consists of three profiles. The profile furthest inland (LINE65) runs NNW–SSE through Teglkær Mose, where the sediment core was taken. The two other profiles (LINE58-59) continue along a path from a road and east towards the coast.

The GPR surveys were carried out using shielded antennas mounted on a hand-pulled skid plate (pulseEKKO PRO® 250 MHz from Sensors and Software) with a spacing of 0.38 m. The step size was 0.053 m, and for each position, eight traces were measured and stacked, each trace consisting of 1000 measurements (one measurement every 0.4 ns for 400 ns). The GPR data were processed using EKKO_Project™ from Sensors and Software. Processing included dewowing, migration, depth conversion and topographic correction. Migration and depth conversion were carried out using constant velocities. Topography data were retrieved from the DEM. The vertical resolution is calculated as one quarter wavelength, corresponding to ~0.1 m.

Optically stimulated luminescence dating

We used OSL dating to constrain the ages of the beach ridges following the procedure used at several sites in Denmark (Bjørnsen *et al.* 2008; Hede *et al.* 2015; Clemmensen *et al.* 2018; Kristiansen *et al.* 2021).

In total, 16 sediment samples were collected; 14 samples were taken along the northern GPR transect and two samples (214508 and 214509) were taken further south, where younger beach ridges are preserved in the upper beach ridge plain (Fig. 1). In locations where the beach ridge deposits were accessible directly at the surface, samples were collected by hand-digging into the shallow subsurface (214501–214509). In the central part of the upper beach ridge system, vegetation and a thick layer of aeolian deposits cover the beach ridges, making sampling of the marine deposits more difficult. Here we dug two 1–2 m deep trenches with a backhoe and took five and two samples respectively (214510–214514 and 214515–214516). All sediment samples for OSL dating were taken in 30-cm-long opaque plastic tubes that were thoroughly sealed with packing tape.

OSL dating was carried out on sand-sized quartz and feldspar grains at the Nordic Laboratory for Luminescence Dating. The OSL measurements on quartz grains were carried out using 8 mm aliquots on stainless steel discs following the SAR protocol (Murray & Wintle 2000, 2003; Murray *et al*. 2021), using a preheat temperature of 160 °C and measuring the OSL at 125 °C. Dose rates were determined using high-resolution gamma spectrometry (Murray *et al*. 2018) and a cosmic ray dose rate contribution based on Prescott & Hutton (1994) and the sampling depth. The dose rate from cosmic radiation in the marine samples may have changed over time owing to the subsequent deposition of aeolian material, but the effect of this change lies well within the dating uncertainty. Samples 214502 and 214503 showed a slow component in the quartz signal resulting in excessively high estimates of D_e (equivalent dose) and were therefore excluded, while for all other quartz samples, it was possible to get a clear, quickly decaying signal. The ability of our chosen protocol to measure a dose in these quartz samples was tested on samples 214504, 214506–214508 and 214510–214516, giving a measured/given ratio of 0.993±0.006 (n = 66), confirming that our protocol can accurately measure a known laboratory dose given before any thermal treatment (Murray 1996).

Infrared stimulated luminescence (IRSL) measurements were carried out on feldspar grains (IR_{50}, stimulation at 50 °C; and $pIRIR_{150}$, stimulation at 150 °C after stimulation at 50 °C) to check whether the OSL signal had been sufficiently reset during deposition. The IRSL signal in feldspar grains is reset more slowly than the OSL signal in quartz grains (Murray *et al*. 2012; Sugisaki *et al*. 2015), and so it can be used to confirm the bleaching of the quartz signal. Dose recovery tests on feldspar samples gave measured/given ratios of 1.030±0.008 ($pIRIR_{150}$) and 1.020±0.013 (IR_{50}), confirming that our IRSL protocol can measure with sufficient accuracy a known laboratory dose given before any thermal treatment.

When referring to ages obtained through different dating methods in the following, OSL ages will be reported in kiloyears before time of sampling (2021 CE) and ^{14}C ages will be reported in cal. ka BP (relative to 1950 CE).

Results

Coastal landforms and dynamics

The compiled geospatial data (Table 1) form a solid base for a preliminary assessment of the coastal landscape evolution at Rugård by providing a reliable indication of the spatial arrangement of landforms. The presence of cliffs eroded into the moraine topography suggest a more exposed state and thus a more landward position of the shoreline at some point prior to the formation of the main succession of Holocene coastal deposits. These deposits are primarily composed of a beach ridge system with a length of 3.5 km and a width of up to 0.8 km. The system is relatively thin at its southern boundary, where the glacial deposits delimit the space for the formation of coastal deposits and becomes progressively wider towards the north, where more accommodation space is available within the pre-Holocene topography. The beach ridge system can be divided into two main units, an upper and a lower system, separated by a marked unconformity (Fig. 1). The upper beach ridges have surface elevations of between 4.5 and 7.5 m across the widest part of the system, where the innermost ridges have elevations of <5 m, whereas the outermost ridges have elevations of >5 m. The ridge crests have an approximate orientation from SSW to NNE and are slightly bent, suggesting the refraction of waves into the bight. Most of the upper beach ridge plain has been covered by a plantation since the late 1800s, and the beach ridges are therefore not easily visible in the landscape, but appear clearly in the DEM. An eroded cliff with an elevation of ~4 m forms a marked unconformity cutting across the beach ridges of the upper system at a low angle. The presence of this erosive landform is a clear indication of a period of coastal retreat and reconfiguration. The unconformity is followed by a lower beach ridge system with an elevation of ~2 m a.s.l. that likewise broadens from south to north and is very similar in structure and orientation to the upper beach ridges.

Analysis of historical maps provides an estimate of changes in shoreline position since *c*. 1780 CE. An important observation is that most of the lower beach ridge plain formed after 1877 CE; at that time only a thin strip of land (~50 m wide) is shown in front of the clearly visible cliff. Since then, the beach ridge plain has prograded in a narrow fan shape, with most progradation occurring at its northern end (just south of the limestone extraction site) (Fig. 1). Between 1877 and 1900 CE, a cross-shore-oriented jetty that served as a harbour was built at the extraction site. Following its construction, the coastline just south of the jetty began to prograde at a rate of ~ 2 m per year averaged over the period until *c*. 1985 CE. Since then, the coastline has been relatively stable with only slight fluctuations in shoreline position.

Sediment core

The 2.74 cm long-core was subdivided into four units based on the lithology, geochemical data and macrofossil content (Fig. 3). The- lower unit 1 (274–184 cm) comprises an upward fining succession of organic-rich sand and silty clay with a relatively high density. At the base, the succession consists of medium-to-coarse sand with high Sr/Ca ratio which gradually changes into light coloured, laminated calcareous silty-clay with a decreasing Sr/Ca ratio. The lower unit contains aquatic plant material (Charophyte) and some molluscs (e.g. *Mytilus*

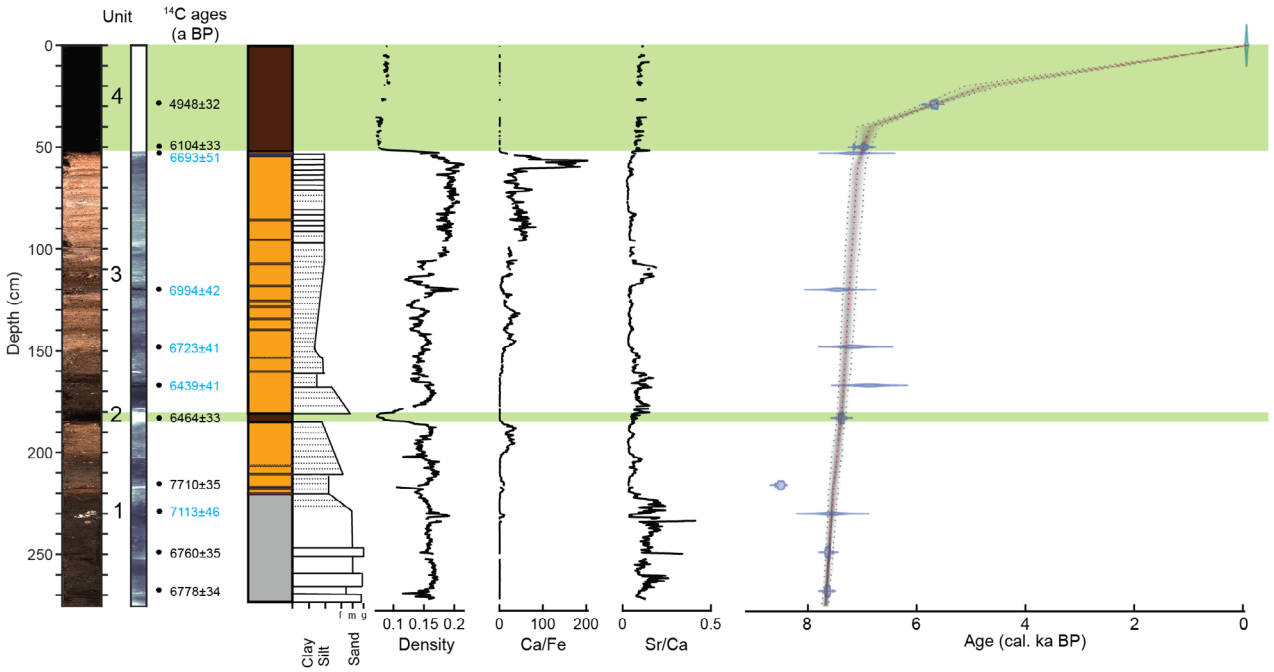

Fig. 3. Lithological, geochemical data and age-depth model of the sediment core from Teglkjær Mose. The core was subdivided into four units based on the lithological changes and macrofossil content. Uncalibrated radiocarbon ages of marine shells (blue) and terrestrial macrofossils (black) are shown next to the lithological log.

edulis, *Parvicardium minimum*, *Hydrobia ventrosa*, *Cerastoderma glaucum*, *Radix peregra* and *Ostracoda*). Unit 2 (184–181) above consists of a thin layer of dark brown peat. The unit has a low density as well as very low Sr/Ca and Ca/Fe ratios. Unit 3 (181–52 cm) consists of light brown, laminated calcareous silty-clay. It has a relatively high density and the Ca/Fe ratio increases towards the top of the unit. It contains aquatic plant macrofossils and numerous molluscs (e.g. *M. edulis*, *P. minimum*, *Cerastoderma* sp., *Rissoa parva*, *Hydrobia ulvae*, *H. ventrosa*, *C. glaucum*, *R. peregra* and *Ostracoda*). The upper unit 4 (52–0 cm) consists of dark brown peat with similar characteristics to unit 2.

Based on the core data, we interpret units 1 and 3 as deposited in brackish water in a lagoonal setting. This is supported by the abundant macrofossils, dominated by brackish water species, although these sections also contain some freshwater and fully marine species indicating varying environmental conditions. The two peat units 2 and 4 are interpreted as deposited in a freshwater bog that was disconnected from the sea.

Using 11 radiocarbon ages from the core, we constructed an age–depth model after excluding one age that is assumed to be too old because of the reworking of organic material (Table 2, Fig. 3). Based on the age–depth model, the lower brackish phase (unit 1) occurred *c*. 7.6 to 7.4 cal. ka BP. It was followed by a short phase of freshwater conditions and peat formation *c*. 7.4 cal. ka BP before returning to brackish water condition again from *c*. 7.4 to 7.0 cal. ka BP. From *c*. 7.0 cal. ka BP until the present, Teglkær Mose was a freshwater bog with no evidence of marine excursions.

Ground-penetrating radar

Good penetration depths of 2–4 m are reached along the entire length of the profiles and distinct radar facies can be identified (Fig. 4). These are interpreted based on the surface geomorphology and ground-truthed using field data (core from Teglkjær Mose, trenches 1 and 2, and the smaller pits dug for OSL sampling). The quality of the GPR data is variable and noisy in parts of the transects, mainly because of the uneven surface and the occasionally dense vegetation in the plantation and across Teglkjær Mose; this negatively affects both the heading and the contact of the antenna/transducer with the sediment surface. Nevertheless, the GPR data provide important information on the internal structure and composition of the coastal deposits.

Along the southern profile (see Figs 1, 4), the moraine surface can be clearly traced as a marked reflection in the shallow subsurface buried below the deposits of Teglkjær Mose and the beach ridges. Locations where moraine topography is visible in the elevation model and the surface geology map are spatially well aligned with the presence of the marked reflection in the GPR data, supporting this interpretation. The onset of beach ridge deposits along the southern profile is characterized by an erosive contact with the moraine deposits, followed by a facies with a pronounced surface topography and clearly

Table 2. Radiocarbon ages from Teglkær Mose, Denmark.

Sample number	Laboratory number	Material	$\delta^{13}C$ (‰)	^{14}C age (a BP)	Modelled age (cal. a BP)		
					Minimum	Maximum	Median
Djurs 28–30	Ua-72627	Wood	−28.0	4948±32	5597	5844	5670
Djurs 49.5–51.5	Ua-72628	Bulk	−29.6	6104±33	6842	7118	6962
Djurs 52–54	Ua-72622	*Cerastoderma glaucum*	−1.6	6693±51	6878	7142	6996
Djurs 120	Ua-72623	*Cerastoderma glaucum*	−2.8	6994±42	7095	7349	7231
Djurs 147–150	Ua-72624	*Cerastoderma glaucum*	0.6	6723±41	7175	7393	7290
Djurs 166–168	Ua-72625	*Mytilus edulis*	2.6	6439±41	7244	7428	7335
Djurs 182–184	Ua-72629	*Terrestrial macrofossil*	−31.0	6464±33	7308	7473	7381
Djurs 215–217	Ua-72630	Grass	−0.5	7710±35	Outlier		
Djurs 228–231	Ua-72626	*Cerastoderma glaucum*	−18.7	7113±46	7475	7628	7550
Djurs 249–250	Ua-72631	Twig	−28.1	6760±35	7529	7663	7598
Djurs 267–269	Ua-72632	Wood	−28.2	6778±34	7589	7715	7645

visible internal reflections dipping towards the coast. Based on their difference in slope, these are interpreted as remnants of the beach profile (beach face and upper shoreface). Downlap points between the two reflection surfaces can here be identified at an elevation of 3.0±0.5 m a.s.l. along the entire succession until the bluff/cliff that marks the transition to the lower beach ridge plain. Across the lower beach ridge plain, signal penetration is relatively low, but reflections are likewise easily identified. No clear sea level estimate could be made, but the surface topography suggests a sea level similar to the present, which corresponds well with the recent formation of the lower beach ridge system, indicated in the analysis of the geospatial data.

Along the northern profile (see Figs 1, 4), the base of the coastal deposits (i.e. the surface of glacial sediments) is not reached. In the innermost part of the profile (LINE66), coastward-dipping reflections are clearly visible, but generally much less distinctive than in the southern profile. The surface topography is relatively flat and the GPR data provide little indication of the processes leading to its formation besides a likely supply of energy and material from the east, suggesting a marine formation. Based on the interpretation of the GPR profile and observations during sampling, RSL at the time of formation is estimated to be ~3 m a.s.l. (RSL estimates at OSL sample locations are listed in Table 3).

The central part of the northern profile is characterized by a marked topography (visible as ridges in the DEM), but no clear dipping direction of the reflections can be identified close to the surface. Based on observations in trenches 1 and 2, these deposits are interpreted as aeolian sand with a weakly marked transition to the marine deposits, both in the trenches and in the GPR data, where coastward-dipping reflections can occasionally be identified at depths of ~1–2 m below the surface (e.g. at trench 1). Past RSL estimates are between 3.7 and 4.5 m a.s.l. across this part of the upper beach ridge plain.

At the unconformity marked by the cliff cutting across the upper beach ridge system, the topography drops by ~4 m accompanied by a marked sloping reflection continuing below the lower beach ridge system, suggesting a much steeper beach profile at the transition between the upper and lower system. Observations in the lower beach ridge plain are similar to those in the southern profile.

OSL dating

A total of 16 samples were dated from the beach ridge system at Rugård, with the aim of providing a robust

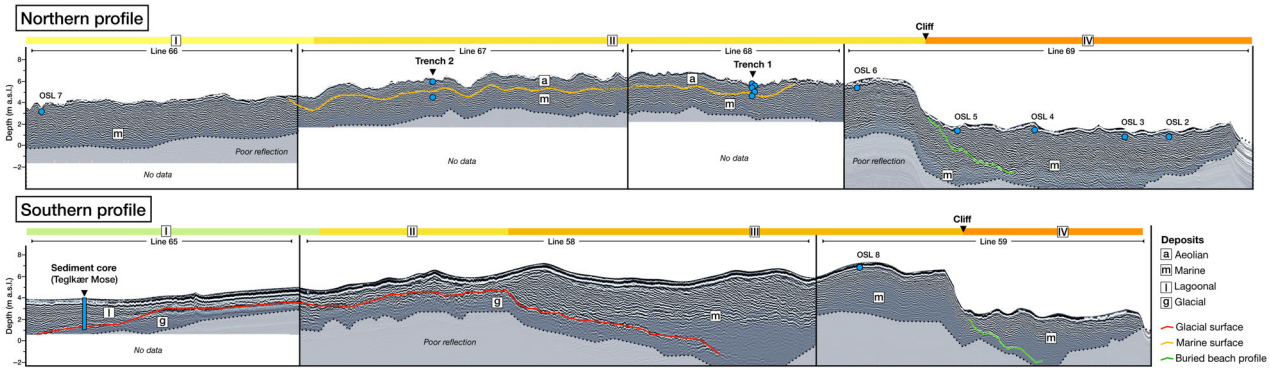

Fig. 4. Overview figure showing the depositional context and main reflections of the two ground-penetrating radar (GPR) profiles recorded at Rugård. The coloured bars correspond to the beach ridge sets identified in Fig. 1.

Table 3. Luminescence ages of the beach-ridge deposits from Rugård (Denmark). Water content (w.c.) is given as a percentage of the total sample weight, and ages are given in ka before sampling year (2021). Quartz optically stimulated luminescence (OSL) ages should be used for interpretation; feldspar IR and pIRIR ages are only used to check quartz OSL bleaching. Missing values indicate that we did not have enough material to measure a D_e (equivalent dose) value or that the sample was excluded owing to a slow component in the quartz signal. Feldspar ages are not corrected for potential signal instability. n_r = number of rejected aliquots; n_a = number of accepted aliquots. Outliers were identified using the interquartile range criterion. All uncertainties in the table are given at 1σ. For the very coarse-grained samples 214504, 214506, 214508 and 214509, the dose rate sample was split into >2 and <2 mm fractions and radionuclide concentrations were measured for both. The β dose rate was calculated based on the assumption that 50% comes from the >2 mm fraction and 50% from the <2 mm fraction. For the γ dose rate component, the contributions were weighted according to the relative weights.

Laboratory code	Sample location	Site	Depth (cm)	w.c. (%)	IR_{50} D_e (Gy)	n_r	n_a	pIRIR D_e (Gy)	n_r	n_a	OSL D_e (Gy)	n_r	n_a	Feldspar dose rate[1] (Gy ka^{-1})	Quartz dose rate (Gy ka^{-1})	IR_{50} age (ka)	pIRIR age (ka)	OSL age (ka)	RSL estimate (m a.s.l.)
214501	1	Rugård	24	2	n.a.			n.a.			n.a.			1.88±0.08	0.94±0.04	n.a.	n.a.	n.a.	0.0±0.5
214502	2	Rugård	19	1	n.a.			n.a.			n.a.			1.76±0.07	0.83±0.04	n.a.	n.a.	n.a.	0.0±0.5
214503	3	Rugård	45	2	n.a.			n.a.			n.a.			1.85±0.08	0.92±0.04	n.a.	n.a.	n.a.	0.0±0.5
214504	4	Rugård	33	1	0.85±0.14	0	9	2.8±0.61	0	8	0.11±0.01	2	28	2.75±0.11	1.72±0.09	0.31±0.05	1.02±0.23	0.07±0.01	0.0±0.5
214505	5	Rugård	18	0	n.a.			n.a.			0.16±0.02	2	15	1.52±0.07	0.58±0.03	n.a.	n.a.	0.28±0.04	0.0±0.5
214506	6	Rugård	68	4	10.65±0.91	0	6	14.64±1.92	0	6	6.7±0.15	1	38	2.16±0.09	1.13±0.06	4.93±0.47	6.78±0.94	5.92±0.34	4.0±0.5
214507	7	Rugård	92	8	12.15±0.62	0	9	15.87±0.82	0	9	8.01±0.15	2	19	2.2±0.09	1.26±0.06	5.53±0.36	7.22±0.49	6.35±0.35	3.0±0.5
214508	8	Rugård	28	2	3.26±0.36	0	8	5.06±1.44	0	5	2.2±0.08	1	28	1.33±0.06	0.68±0.03	2.45±0.30	3.81±1.10	3.22±0.20	3.0±0.5
214509	9	Rugård	35	1	3.78±0.92	0	3	5.38±1.83	0	3	2.17±0.14	1	20	1.99±0.12	0.96±0.10	1.9±0.48	2.7±0.94	2.25±0.27	No GPR
214510	Trench 1	Rugård	138	7[2]	10.15±0.49	0	9	12.62±0.51	0	9	6.76±0.15	1	23	1.97±0.08	1.03±0.05	5.16±0.31	6.41±0.39	6.56±0.37	3.7±0.5
214511	Trench 1	Rugård	114	7[2]	9.66±0.59	1	5	11.72±0.95	0	6	6.25±0.17	1	28	1.93±0.08	0.99±0.05	5.01±0.37	6.07±0.57	6.3±0.36	3.7±0.5
214512	Trench 1	Rugård	48	7[2]	3.22±0.11	3	9	5.06±0.26	0	12	2.43±0.04	4	26	1.79±0.07	0.85±0.04	1.8±0.10	2.82±0.19	2.85±0.15	Aeolian
214513	Trench 1	Rugård	28	13	0.72±0.02	1	8	0.97±0.02	1	8	0.39±0.01	1	29	1.85±0.07	0.91±0.04	0.39±0.02	0.52±0.03	0.43±0.02	Aeolian
214514	Trench 1	Rugård	21	16	2.19±0.37	0	9	3.31±0.60	0	9	1.05±0.08	2	22	1.8±0.07	0.86±0.03	1.22±0.21	1.84±0.35	1.21±0.11	Aeolian
214515	Trench 2	Rugård	167	8[2]	10.55±0.54	1	8	14.38±0.41	1	8	7.32±0.17	0	30	2.15±0.09	1.21±0.06	4.9±0.32	6.69±0.36	6.04±0.35	4.0±0.5
214516	Trench 2	Rugård	25	8[2]	4.18±0.68	1	5	6.55±0.52	1	5	3.19±0.19	0	36	2.05±0.08	1.11±0.05	2.04±0.34	3.19±0.29	2.87±0.22	Aeolian

[1]Feldspar dose rates include an internal β dose rate component from K-40 amounting to 0.857±0.041 Gy ka^{-1}.
[2]Calculated as 20% of saturated water content.

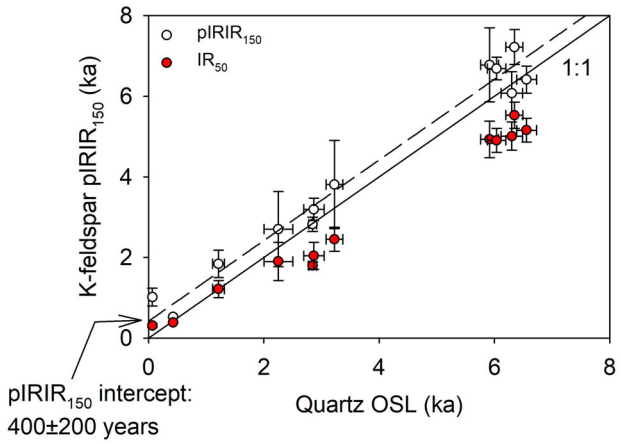

Fig. 5. Comparison of optically stimulated luminescence (OSL) dates obtained from quartz and feldspar (IR_{50} and $pIRIR_{150}$) samples.

chronology for the formation of both the beach deposits and the aeolian deposits covering them. Table 3 and Fig. 5 show the results of OSL dating of quartz in comparison with the results determined from OSL dating of feldspar (IR_{50} and $pIRIR_{150}$). The IR_{50} ages are generally lower than the quartz ages, and the $pIRIR_{150}$ ages generally agree well with the quartz ages with an offset of a few hundred years, indicating that the quartz grains were almost certainly well bleached before final deposition.

The ages show that the marine deposits in the upper part of the system formed over a period of a few hundred years between 6.56±0.37 and 5.92±0.34 ka ago (samples 214506–214507, 214510–214511 and 214515). These ages are in relatively good agreement and have overlapping uncertainties. The two samples from the outermost (southern) part of the upper beach ridge system have ages of 3.22±0.20 and 2.25±0.27 ka. These ages are significantly younger and suggest a reduction in progradation rate.

Aeolian samples from trenches 1 and 2 are dated between 2.87±0.22 and 0.43±0.02 ka. There is a significant age inversion in the topmost two samples in trench 1. Given that the IRSL ages are consistent with those from quartz (indicating that the quartz was well bleached at deposition), this may reflect gross physical disturbance, perhaps in relation to the plantation.

The samples from the lower part of the beach ridge system yield ages of 0.07±0.01 and 0.28±0.04 ka (*c.* 1950 and 1740 CE).

Discussion

Landscape evolution at Rugård

Based on the overall results, the landscape formation of the coastal depositional system at Rugård is divided into six distinct phases (Fig. 6A–F), described in the following sections.

Transgression and lagoonal deposits (c. 7.6–7.0 cal. ka BP). – Dating and interpretation of the sediment core indicate that Teglkær Mose was initially a shallow brackish lagoon from at least around *c.* 7.6 cal. ka BP. A calcareous silty clay intercalated with sand interbeds was deposited in the lagoonal environment. Calm conditions are a prerequisite for the deposition of cohesive sediment. The formation of a barrier separating the topographic depression of the bog from the open marine environment must thus have occurred prior to the formation of the lagoonal deposits (Fig. 6B). In the elevation model, a hummocky signature south of the bog suggests the presence of till at the surface, while a visible palaeo-cliff/bluff in one moraine hill suggests local wave erosion and coastal retreat that could have supplied the sediment necessary for the construction of a coastal barrier. This can be further supported by the presence of a small cliff at a similar location in the moraine deposits (visible in GPR LINE58) covered by >2 m of marine sand and gravel deposited on top of the erosive contact.

The lagoonal basin rapidly filled up over a period of *c.* 700 years. Two peat layers dated to *c.* 7.4 and 7.0 cal. ka BP suggest periods of basin freshening or reduced marine influence. After deposition of the lower peat layer, renewed deposition of calcareous silty clay suggests a second period of increased marine influence. The fossil content and lack of sand inclusions further up in the core suggest that the connection between the marine environment and the lagoon was increasingly restricted towards *c.* 7.0 cal. ka BP, when the second phase of peat formation began.

The time window for deposition is in good agreement with a transgressive stage, characterized by high rates of RSL rise, documented in other coastal systems across the southern Kattegat (Hede 2003; Sander *et al.* 2015a). It must be assumed that erosion of the moraine both north and south of Teglkær Mose (marked with black lines in Fig. 6A) was associated with the marked rise in RSL. Erosion products from the moraine may have been transported northward and have formed the first beach ridges, cutting off Teglkær Mose from the marine environment. Large amounts of sediment must have been mobilized and transported into the bay during this transgressive stage and may have facilitated the formation of the initial beach ridges in the area. The age and thickness of the innermost sand deposits of the bay are unknown (set I in Fig. 1), but their elevation and position in the back-barrier of the upper beach ridge system suggest an early (Middle Holocene) formation.

Relative sea level highstand and beach ridge formation (c. 6.6–5.9 ka ago). – The OSL ages obtained from the upper beach ridge system suggest that formation occurred relatively quickly over the period between *c.* 6.6 and 5.9 ka ago (set II in Figs 1, 6C). This suggests a large supply of sediment to the area. The timing of deposition is in agreement with the ages suggested for the

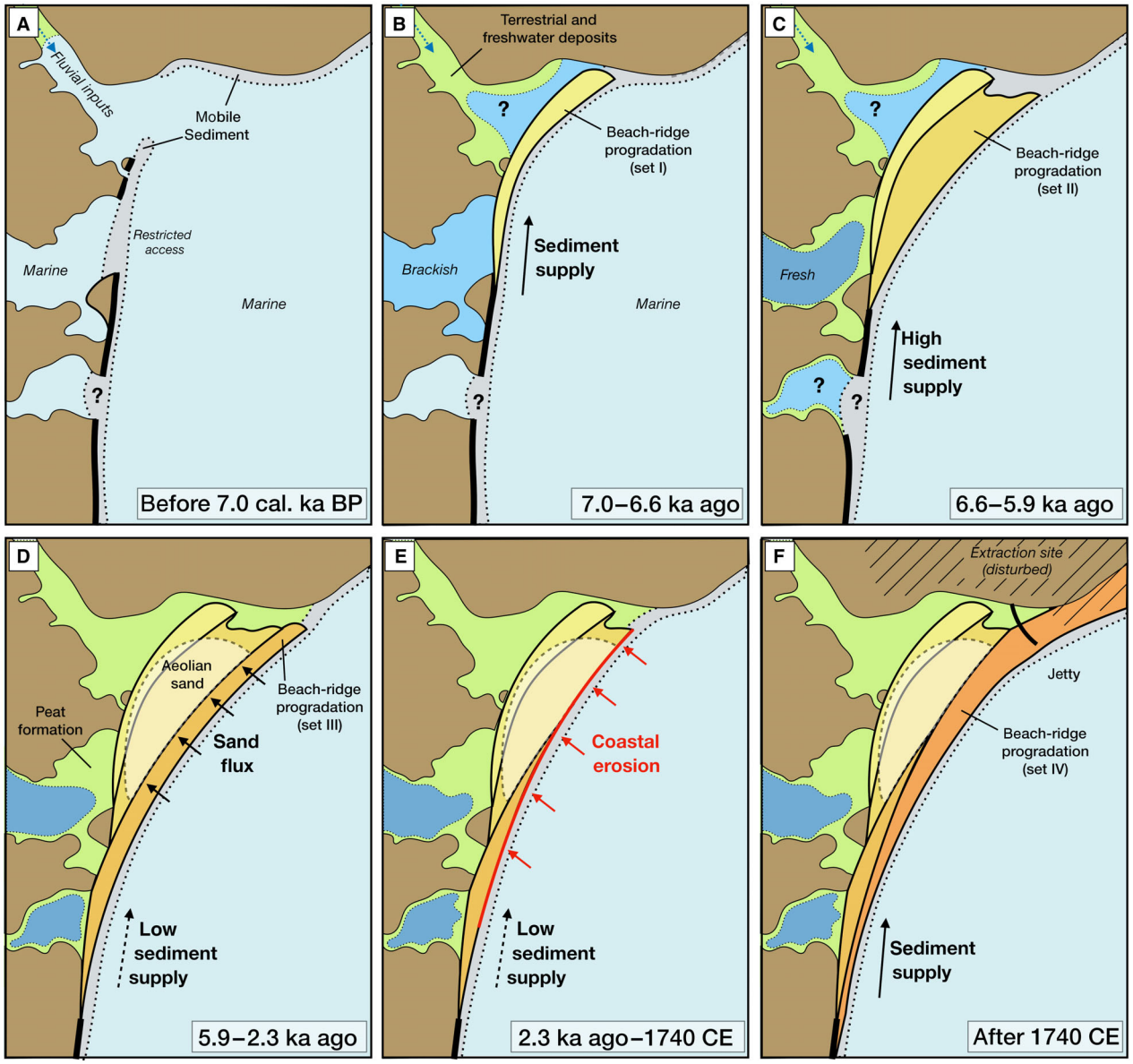

Fig. 6. Schematic model of the Middle and Late Holocene landscape evolution at Rugård. A. Transgression and mobilization of sediment by coastal processes. B. Relative sea-level highstand, initial barrier formation and lagoonal deposition at Teglkær Mose. C. Rapid beach-ridge progradation. D. Formation of beach ridges (slow progradation) and influx of aeolian sediment on the older beach deposits. E. Coastal erosion and formation of the unconformity (cliff). F. Formation of the lower beach ridge system.

stabilization of the global, post-glacial sea level rise (Fleming *et al.* 1998) and stabilization of regional RSL, which reaches its maximum around this time (Christensen & Nielsen 2008; Sander *et al.* 2016; Bennike *et al.* 2021).

The coastal system at Rugård is located in the apex of a bay between two pronounced cliffed headlands, suggesting significant erosion of the moraine deposits and hence a potentially large supply of sediment from a local source. Likewise, the large-scale geomorphology of the shoreline of eastern Djursland (Fig. 1) suggests ample longshore transport. Along the first ~350 m of the northern GPR transect, the surface elevation of the beach ridges rises towards the coast, which confirms the idea that the coastal development in this period has primarily been driven by sediment input (Figueiredo & Rockwell 2022) and has not occurred as a forced regression owing to RSL fall. Interpretation of the GPR profiles actually indicates a RSL rise to ~4.5 m a.s.l. followed by a fall of ~0.5 m within the period of deposition. The estimated sea level thus follows the overall topography of the beach ridge system, which is also the case in similar studies from Anholt and Samsø (Clemmensen *et al.* 2012; Hede *et al.* 2015). Human settlements and shells from molluscs far within Kolindsund (north of Rugård) and towards

Stubbe Sø (south of Rugård) confirm a high RSL during this period (Pedersen & Petersen 1997).

The absence of marine deposits in the sediment core from Teglkær Mose at this time may be explained by the presence of a barrier shielding the bog from the sea, or by the fact that the peat in Teglkær Mose was formed at a higher elevation and subsequently compacted and sank to the level where we find it today. Teglkær Mose was drained before 1811 CE (Parish map), and the drainage system was later expanded to its current form, which has probably led to compaction.

The youngest dated beach deposits from the central part of the upper beach ridge plain (set II in Fig. 1; OSL 6, sample dated to *c*. 5.9 ka) and the younger beach ridges further south (OSL 8 and 9) are much coarser than the older deposits and contain large quantities of pebble- and cobble-sized material. This is interpreted as an indication of an equilibrium state in coastal configuration (aided by a falling RSL trend), where the massive sediment supply has led to an alignment of the shoreline and thus a situation where longshore transport (of primarily sand- and gravel-sized particles) outweighs the infilling of the remaining accommodation space. As a result, deposition is increasingly dominated by reworking of the beach sediments, leading to the deposition of predominantly coarse particles within the beach ridges.

Younger beach ridges in the upper plain (c. 3.2–2.3 ka ago). – Despite pronounced erosion in the northern part of the system, two coarse-grained beach ridges (clasts up to ~3 cm) in the upper plain have been preserved in the southern part of the area (set III, Fig. 1). They are dated to *c*. 3.2 ka (OSL 8) and *c*. 2.3 ka (OSL 9), which is considerably younger than the beach ridges slightly further inland, and a surprisingly young age given the surface topography of the beach ridges (6.8 and 6.4 m a.s.l., respectively).

Downlapping reflections below OSL 8 (corresponding to the extension of the dated beach face reflector) suggest a RSL at around 3.0±0.5 m a.s.l. at the time of formation. This is somewhat high and somewhat young within the framework of sites studied in the Danish Holocene coastal environment, but not too far off from estimates for the sea level height and timing towards the end of the Middle Holocene RSL highstand (Clemmensen *et al*. 2012; Hede *et al*. 2015; Sander *et al*. 2016). For OSL 9, there is no indication of RSL based on GPR.

It is interesting to note that the transition from sand- to clast-dominated beach deposits indicates a major influence of beach morphodynamics. Both GPR profiles resolve a marked reflection in continuation of the cliff/bluff separating the upper and lower beach ridge system. This suggests a much steeper beach profile, indicating a high degree of reworking and a dominance of coarse clastic material both on the beach face and on the upper shoreface (Orford *et al*. 1991). Furthermore, along beach ridge systems where RSL indicators can be obtained from downlapping reflections along the entire profile, both a detachment in the elevation of topography and downlap points and a certain degree of variability in their elevation (~±0.5 m) within shorter time-windows can be observed (Hede *et al*. 2015).

Ultimately, the observed ages and RSL elevations of beach ridges in set III (Fig. 1) have indicative value, but a high degree of uncertainty remains, and the system requires further investigation. For the strand plain at Rugård overall, a marked change in the pattern of progradation can be identified between sets II and III (Fig. 1) that probably relates to local changes in sediment supply and possibly wave energy.

Sand drift (c. 2.9 ka ago to present). – The central part of the upper beach ridge plain is covered by aeolian sand, and OSL ages suggest a pronounced period of sand drift *c*. 2.9–2.8 ka ago (Fig. 6D). The GPR profiles show slightly eastward-sloping reflections, so the sand was probably deposited by easterly winds, suggesting a marine source of the deposits (i.e. the beach).

Two OSL samples give ages of 1.2 and 0.4 ka, which suggests that aeolian deposition has occurred more or less continuously since *c*. 2.9 ka ago. Nothing in the GPR data suggests the formation or mobility of dunes, which indicates an influx of sand into a sparsely vegetated coastal landscape. Over time, a layer of aeolian sand with a thickness of up to 1.5 m was deposited on top of the beach deposits.

Coastal erosion (c. 2.3 ka to c. 1740 CE). – At some point after the formation of the upper beach ridge plain, a period of erosion of the coast occurred (Fig. 6E). The progradation rates of the beach ridges declined markedly after *c*. 5.9 ka ago and stayed low until at least *c*. 2.3 ka ago, after which a clearly visible cliff was formed, cutting obliquely at a low angle across the main orientation of the beach ridges. Overall, the cliff is more pronounced in the northern part of the system than in its southern part. Erosion surfaces are visible in the GPR data below the deposits of the lower beach ridge plain. The erosion surface in the southern GPR profile is slightly more inclined and the overall geometry in the arrangement of landforms suggests a slight rotation, which is supported by the proximity of till in the shallow subsurface. This suggests that a marked reduction in sediment transport upcurrent may have led to sediment starvation downcurrent, causing a shift in the beach ridge system to a phase of coastal retreat.

Formation of the lower beach ridge system (after c. 1740 CE). – A renewed period of progradation then led to the formation of the lower beach ridge plain (Fig. 6F). The map analysis indicates that the lower beach deposits formed after 1780 CE (Parish map), which is consistent with OSL 5, providing an age of 1740±40 CE.

As expected, the topography and internal structure of the beach ridges show no signs of RSL changes during this period. The shift from erosion to new progradation can probably be explained by the construction of a pier for shipping of materials from the extraction site north of the beach ridge system that acted as a sediment trap and prevented further longshore sediment transport. The Danish Coastal Atlas (Danish Coastal Authority 2010) indicates continued progradation of the beach ridge plain, while the coast south of the area is being eroded.

Drivers of coastal landscape evolution and regional outlook

Relative sea level. – The general course of the regional Holocene RSL history is well constrained by previous studies from the southern Kattegat (Hede *et al.* 2015; Sander *et al.* 2015a, b, 2016; Bennike *et al.* 2021) and from other coastal areas of central Denmark (Christensen 1982; Clemmensen *et al.* 2012). A short period of pronounced RSL rise around 7.7–7.5 ka ago led to the establishment of a highstand period at around 6.5 ka ago that lasted until *c.* 4.0 ka ago, when a marked drop in RSL is documented at several sites across central Denmark (Christensen 1982; Clemmensen *et al.* 2012, 2018; Hede *et al.* 2015; Sander *et al.* 2016). Over the following millennia, the development was primarily determined by a slow RSL fall driven by isostatic uplift. Overall, Denmark is largely impacted by glacial-isostatic adjustment that causes a strong regional variability in uplift rates (Rosentau *et al.* 2021). While the general pattern of uplift has already been constrained in early studies (Mertz 1924), there is a growing body of evidence that regional variations and temporal changes in uplift rates may be more pronounced than previously assumed (Vestøl *et al.* 2019; Rosentau *et al.* 2021).

Most of the dated marine deposits from this study formed in the relatively short time period between *c.* 7.6 cal. ka BP and 5.9 ka ago and it is hence not possible to compile a continuous Holocene RSL reconstruction from the preserved depositional sequences at Rugård (Fig. 7). Nevertheless, several of the observations are linked to changes in coastal forcing and RSL.

The first deposits at Teglkjær Mose were dated to *c.* 7.6 cal. ka BP and hence are in good agreement with the expected timing of the marine transgression in the area. The contact between the Pleistocene till and the Holocene coastal deposits is not included in the core, but the ages, the properties of the deposits and the GPR data (LINE65) suggest that the base of the core must have been in proximity to the pre-Holocene surface. As discussed earlier, the deposition of organic matter and fine-grained material is conditional upon the establishment of calm conditions, which in turn require the formation of a barrier separating the lake basin from open marine conditions. Evidence of barrier (spit) formation at a suitable location and elevation is visible

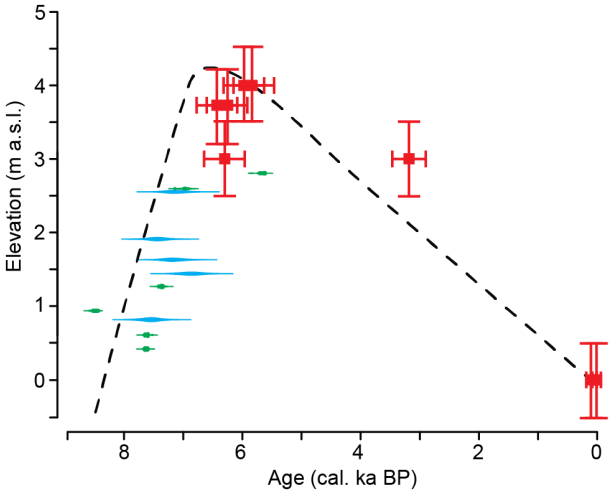

Fig. 7. Relative sea level curve for Rugård (stippled line) based on radiocarbon ages from marine (blue) and lacustrine (green) sediments from Teglkær Mose, and OSL ages of relative sea level estimates obtained through GPR in beach ridges (red). The curve is placed above all the radiocarbon ages because the succession of peat and marine deposits was compacted when the bog was drained in the 1800s.

in the DEM, and erosive features on a minor elevation of the moraine are visible both in the DEM and in the GPR data (LINE58). Rapid sedimentation in Teglkjær Mose continues until *c.* 7.0 cal. ka BP and coincides well with the OSL age obtained on the innermost visible beach ridge of the upper system (*c.* 6.3 ka). This means that the initiation of beach ridge progradation occurs at approximately the same time as Teglkjær Mose is fully separated from marine influence and at about the same time when the stabilization of RSL has been proposed in other studies from Denmark (Bjørnsen *et al.* 2008; Christensen & Nielsen 2008; Clemmensen *et al.* 2018). Downlapping reflections in GPR LINE66 suggest that RSL at that time has been at an elevation of 3.0 m a.s.l. Bennike *et al.* (2021) present a single data point on marine deposits from the island of Hjelm (see Fig. 7) that are located at an elevation of 3.8 m a.s.l. and were dated to *c.* 5.9 cal. ka BP, which agrees well with the results from this study. It should be added, however, that Bennike *et al.* (2021) suggest that the deposits on Hjelm may have formed during a storm.

Progradation and sediment supply. – While the role of RSL in explaining changes in the landscape at Rugård is relatively apparent in the early stages of coastal evolution, the indications become much less clear after *c.* 5.9 ka ago. The OSL ages of the marine deposits in the upper beach ridge plain suggest that a succession with a width of >0.5 km formed within the uncertainty of the dating method, which roughly corresponds to an averaged progradation rate of >1 m a^{-1}. The uncertainty on the age indication (and hence on the progradation rates) is relatively high, but this figure provides a solid indication that the system formed over a

relatively short period and as a result of massive sediment supply (rather than forced regression). Similarly high progradation rates have been documented from other beach ridge systems and were usually explained by a mix of exposure to wave energy, sediment availability, and the presence of accommodation space (e.g. Hein *et al*. 2013; Sander *et al*. 2015a, b, 2019; Oliver *et al*. 2020). At some point after *c*. 5.9 ka ago, the system shifted to a much slower rate of progradation (or to alternating periods of stability and progradation). Two OSL samples from the southern part of the system yielded ages of *c*. 3.2 and 2.3 ka and thus point to a pronounced decline in the overall progradation rate to ~3 m per century over a time period of *c*. 3600 years.

Anthropogenic changes and climate. – The construction of a jetty (around 1900 CE) for the shipping of material from the extraction site just north of the beach ridge system appears to have had a significant influence on the local sediment budget of the beaches at Rugård. The jetty is positioned in a cross-shore direction with regard to the orientation of the beach, which, under a situation of main wave energy supply from the south, leads to an effective increase in accommodation space. After 1900 CE, the lower beach ridge system prograded roughly 120 m until the mid-1980s, which corresponds to a progradation rate of ~1.4 m a^{-1} and thus in a similar order of magnitude as the Middle Holocene rates of beach progradation. This further supports the assumption that deposition of sediment on beaches at Rugård became limited by the lack of accommodation and that the erosive unconformity observed in the system (between the upper and lower beach ridge system) may have resulted from a period of restricted sediment supply that brought the system out of equilibrium – hence causing erosion downcurrent. Potential triggers for a reduction of sediment input along the east coast of Djursland could be changes in the wind field and thus changes in the wave energy budget at Rugård, leading to a reduced sediment delivery. It is worth noting that two large beach ridge plains (Gåsehage, Ahl) formed at an elevation lower than the upper beach ridges and higher than the lower ridges, suggesting that their formation may have occurred during a period when no sedimentation occurred at Rugård.

Conclusions

In this study, we used a multiproxy approach to study the Holocene RSL changes and coastal evolution at Rugård in central Denmark. We find that the beach ridge system at Rugård formed in distinct stages during the period of RSL highstand and fall over the Middle and Late Holocene, controlled by changes in accommodation space (caused by RSL changes or anthropogenic alterations of the coastline) and changes in sediment supply. Between progradation phases, long periods of reworking/erosion occurred, when sediment supply and/or accommodation space was limited. Following a transgression *c*. 7.6 cal. ka BP, the upper beach ridge plain was deposited *c*. 6.6–5.9 ka ago during a highstand period with a maximum RSL of ~4.5 m a.s.l. The following period is not well represented in deposits at Rugård, but a few marked, coarse-grained beach ridges indicate a long period of reworking of the coastline until around 2.3 ka ago, followed by a period of erosion and coastal retreat especially in the northern part of the area, probably caused by reduction in sediment transport upcurrent. Since *c*. 1740 CE, renewed progradation has taken place, forming the lower beach ridge plain. No evidence of RSL changes is visible in these deposits, and the formation is at least partly attributed to the construction of a jetty downcurrent, creating new accommodation space. Aeolian deposits covering the highest part of the beach ridge plain yield ages of up to *c*. 2.9 ka and suggest a more or less continuous influx of aeolian sand from the beach. The new results from Rugård raise some questions about the sea-level development around 3.2–2.3 ka ago, where our data indicate a relatively high RSL position for this time compared with other locations in Denmark. However, the data are not sufficient to say anything definitive in this regard. Overall, our results from Rugård confirm previous estimates of the level and timing of maximum Holocene RSL and contribute to the joint knowledge and understanding of coastal dynamics and landscape evolution under varying conditions in the Middle and Late Holocene.

Acknowledgements. – We thank Jens Reddersen from Mols Bjerge National Park for advice and logistical support. Landlord Elisabeth Mourier-Petersen and forest manager Søren Nørgaard Madsen from Rugård Gods are thanked for permission to work on the property and logistical support. We thank Svend Funder and Anthony Ruter for helping identify the marine molluscs and terrestrial and aquatic macrofossils used for the ^{14}C dating, respectively. Marie-Louise Siggaard-Andersen is thanked for her help and advice concerning the XRF core scanning, and Warren Thompson and Henrik Olesen for their help preparing the OSL samples for measurements. Funding for the project was provided by Mols Bjerge National Park. We would like to thank S. Yeong Bae and one anonymous reviewer for their constructive comments and feedback on our manuscript.

Author contributions. – MHR and NKL conceived the research idea, MHR, NKL, LS and LN conducted the fieldwork, MHR and NKL dated and analysed the sediment core, MHR, LN and LS processed and interpreted the GPR. MHR, AJMC and J-PB dated the beach ridges using OSL. All co-authors contributed to the interpretation of the data. MHR, LS and NKL wrote the first draft of the manuscript. All co-authors have contributed to and accepted the final version of the manuscript.

Data availability statement. – The data that support the findings of this study will be made openly available in the PANGAEA database (https://pangaea.de/).

References

Bennike, O., Andresen, K. J., Astrup, P. M., Olsen, J. & Seidenkrantz, M.-S. 2021: Late Glacial and Holocene shore-level changes in the

Aarhus Bugt area, Denmark. *GEUS Bulletin 47*, 6530, https://doi.org/10.34194/geusb.v47.6530.
Bennike, O., Nørgaard-Pedersen, N., Jensen, J. B., Andresen, K. J. & Seidenkrantz, M.-S. 2019: Development of the western Limfjord, Denmark, after the last deglaciation: a review with new data. *Bulletin of the Geological Society of Denmark 67*, 53–73.
Bjørnsen, M., Clemmensen, L. B., Murray, A. & Pedersen, K. 2008: New evidence of the Littorina transgressions in the Kattegat: optically stimulated luminescence dating of a beach ridge system on Anholt, Denmark. *Boreas 37*, 157–168.
Blaauw, M. & Christen, J. A. 2011: Flexible paleoclimate age-depth models using an autoregressive gamma process. *Bayesian Analysis 6*, 457–474.
Christensen, C. 1982: Havniveauændringer 5500–2500 f. Kr. i Vedbækområdet, NØ-Sjælland. *Dansk Geologisk Forening Årsskrift 1981*, 91–107.
Christensen, C. & Nielsen, A. B. 2008: Dating Littorina sea shore levels in Denmark on the basis of data from a Mesolithic coastal settlement on Skagens Odde, northern Jutland. *Polish Geological Institute Special Papers 23*, 27–38.
Clemmensen, L. B., Hougaard, I. W., Murray, A. S. & Pedersen, S. S. 2018: A high-resolution sea-level proxy dated using quartz OSL from the Holocene Skagen Odde spit system, Denmark. *Boreas 47*, 1184–1198.
Clemmensen, L. B., Murray, A. S. & Nielsen, L. 2012: Quantitative constraints on the sea-level fall that terminated the Littorina Sea stage, southern Scandinavia. *Quaternary Science Reviews 40*, 54–63.
Croudace, I. W. & Rothwell, R. G. 2015: *Micro-XRF Studies of Sediment Cores – Applications of a Non-destructive Tool for the Environmental Sciences.* 649 pp. Springer, Dordrecht, Heidelberg, New York, London.
Danish Coastal Authority 2010: *Kystatlas.* Available at: https://geodata-info.dk/srv/dan/catalog.search#/metadata/af0fd970-b278-486e-a9d5-0df08e460081 (accessed 20.02.2022).
Danish Geodata Agency 2023: *Historiske kort på nettet*. Available at: https://hkpn.gst.dk/ (accessed 26.07.2023).
Dataforsyningen 2023: *Dataoversigt*. Available at: https://dataforsyningen.dk/data (accessed 24.07.2023).
Figueiredo, P. M. & Rockwell, T. 2022: 2.17 - Application of coastal landforms to active tectonic studies. *In* Shroder, J. F. (ed.): *Treatise on Geomorphology*, 443–476. Academic Press.
Fleming, K., Johnston, P., Zwartz, D., Yokoyama, Y., Lambeck, K. & Chappell, J. 1998: Refining the eustatic sea-level curve since the Last Glacial Maximum using far- and intermediate-field sites. *Earth and Planetary Science Letters 163*, 327–342.
Fruergaard, M., Møller, I., Johannessen, P. N., Nielsen, L. H., Andersen, T. J., Nielsen, L., Sander, L. & Pejrup, M. 2015: Stratigraphy, evolution, and controls of a Holocene transgressive–regressive barrier island under changing sea level: Danish North Sea coast. *Journal of Sedimentary Research 85*, 820–844.
GEUS 2023: *Geological surface map of Denmark 1:25.000*. Available at: https://data.geus.dk/geonetwork/srv/eng/catalog.search#/metadata/4ff905e0-f1cf-4906-8a71-1133b346cbb9?lang=da (accessed 31.07.2023).
Hansen, J. M., Aagaard, T. & Binderup, M. 2012: Absolute sea levels and isostatic changes of the eastern North Sea to central Baltic region during the last 900 years: sea level changes in the last 900 years, eastern North Sea. *Boreas 41*, 180–208.
Harder, P. 1908: En Østjydsk Israndslinie og dens Indflydelse paa Vandløbene. *Danmarks Geologiske Undersøgelse II*, 1–227.
Heaton, T. J., Kohler, P., Butzin, M., Bard, E., Reimer, R. W., Austin, W. E. N., Ramsey, C. B., Grootes, P. M., Hughen, K. A., Kromer, B., Reimer, P. J., Adkins, J., Burke, A., Cook, M. S., Olsen, J. & Skinner, L. C. 2020: Marine20-the marine radiocarbon age calibration curve (0-55,000 cal BP). *Radiocarbon 62*, 779–820.
Hede, S. U. 2003: Prehistoric settlements and Holocene relative sea-level changes in northwest Sjælland, Denmark. *Bulletin of the Geological Society of Denmark 50*, 141–149.
Hede, M. U., Bendixen, M., Clemmensen, L. B., Kroon, A. & Nielsen, L. 2013: Joint interpretation of beach-ridge architecture and coastal topography show the validity of sea-level markers observed in ground-penetrating radar data. *The Holocene 23*, 1238–1246.
Hede, M. U., Sander, L., Clemmensen, L. B., Kroon, A., Pejrup, M. & Nielsen, L. 2015: Changes in Holocene relative sea-level and coastal morphology: a study of a raised beach ridge system on Samsø, southwest Scandinavia. *The Holocene 25*, 1402–1414.
Heier-Nielsen, S., Conradsen, K., Heinemeier, J., Knudsen, K. L., Nielsen, H. L., Rud, N. & Sveinbjornsdottir, A. E. 1995: Radiocarbon dating of shells and foraminifera from the Skagen Core, Denmark: evidence of reworking. *Radiocarbon 37*, 119–130.
Hein, C. J., Fitzgerald, D. M., Cleary, W. J., Albernaz, M. B., de Menezes, J. T. & Klein, A. H. D. F. 2013: Evidence for a transgressive barrier within a regressive strandplain system: implications for complex coastal response to environmental change. *Sedimentology 60*, 469–502.
Houmark-Nielsen, M. 2011: Pleistocene glaciations in Denmark: a closer look at chronology, ice dynamics and landforms. *In* Ehlers, J., Gibbard, P. L. & Hughes, P. D. (eds.): *Developments in Quaternary Sciences 15*, 47–58. Elsevier, Amsterdam.
Houmark-Nielsen, M. & Kjær, K. H. 2003: Southwest Scandinavia, 40-15 kyr BP: palaeogeography and environmental change. *Journal of Quaternary Science 18*, 769–786.
Kristiansen, S. M., Ljungberg, T. E., Christiansen, T. T., Dalsgaard, K., Haue, N., Greve, M. H. & Nielsen, B. H. 2021: Meadow, marsh and lagoon: late Holocene coastal changes and human–environment interactions in northern Denmark. *Boreas 50*, 279–293.
Larsen, G. & Knudsen, B. 1983: Geologiske forhold under havbunden ud for Glatved ved Djurslands østkyst. *Dansk Geologisk Forening Årsskrift 1982*, 27–33.
Larsen, N. K., Knudsen, K. L., Krohn, C. F., Kronborg, C., Murray, A. S. & Nielsen, O. B. 2009: Late Quaternary ice sheet, lake and sea history of southwest Scandinavia – a synthesis. *Boreas 38*, 732–761.
Mertz, E. L. 1924: Oversigt over de sen-og postglaciale niveauforandringer i Danmark. *Danmarks Geologiske Undersøgelse. II. Række 41*, 1–50.
Murray, A. S. 1996: Developments in optically stimulated luminescence and photo-transferred thermoluminescence dating of young sediments: application to a 2000 year sequence of flood deposits. *Geochimica et Cosmochimica Acta 60*, 565–576.
Murray, A. S. & Wintle, A. G. 2000: Luminescence dating of quartz using an improved single-aliquot regenerative-dose protocol. *Radiation Measurements 32*, 57–73.
Murray, A. S. & Wintle, A. G. 2003: The single aliquot regenerative dose protocol: potential for improvements in reliability. *Radiation Measurements 37*, 377–381.
Murray, A. S., Arnold, L. J., Buylaert, J.-P., Guérin, G., Qin, J., Singhvi, A. K., Smedley, R. & Thomsen, K. J. 2021: Optically stimulated luminescence dating using quartz. *Nature Reviews Methods Primers 1*, 72, https://doi.org/10.1038/s43586-021-00068-5.
Murray, A. S., Helsted, L. M., Autzen, M., Jain, M. & Buylaert, J. P. 2018: Measurement of natural radioactivity: calibration and performance of a high-resolution gamma spectrometry facility. *Radiation Measurements 120*, 215–220.
Murray, A. S., Thomsen, K. J., Masuda, N., Buylaert, J. P. & Jain, M. 2012: Identifying well-bleached quartz using the different bleaching rates of quartz and feldspar luminescence signals. *Radiation Measurements 47*, 688–695.
Nielsen, L. & Clemmensen, L. B. 2009: Sea-level markers identified in ground-penetrating radar data collected across a modern beach ridge system in a microtidal regime. *Terra Nova 21*, 474–479.
Oliver, T. S., Tamura, T., Brooke, B. P., Short, A. D., Kinsela, M. A., Woodroffe, C. D. & Thom, B. G. 2020: Holocene evolution of the wave-dominated embayed Moruya coastline, southeastern Australia: sediment sources, transport rates and alongshore interconnectivity. *Quaternary Science Reviews 247*, 106566, https://doi.org/10.1016/j.quascirev.2020.106566.
Olsen, J., Kjær, K. H., Funder, S., Larsen, N. K. & Ludikova, A. 2012: High-Arctic climate conditions for the last 7000 years inferred from multi-proxy analysis of the Bliss Lake record, North Greenland. *Journal of Quaternary Science 27*, 318–327.

Olsson, I. U. 1980: Content of ^{14}C in marine mammals from northern Europe. *Radiocarbon 22*, 662–675.
Orford, J. D., Carter, R. W. & Jennings, S. C. 1991: Coarse clastic barrier environments: evolution and implications for Quaternary sea level interpretation. *Quaternary International 9*, 87–104.
Pedersen, S. A. S. & Petersen, K. S. 1997: *Djurslands Geologi*. 96 pp. Geografforlaget, Brenderup.
Prescott, J. R. & Hutton, J. T. 1994: Cosmic ray contributions to dose rates for luminescence and ESR dating: large depths and long-term time variations. *Radiation Measurements 23*, 497–500.
Reimer, P. J. and 41 others 2020: The Intcal20 Northern Hemisphere radiocarbon age calibration curve (0–55 cal kBP). *Radiocarbon 62*, 1–33.
Rosentau, A., Klemann, V., Bennike, O., Steffen, H., Wehr, J., Latinović, M., Bagge, M., Ojala, A., Berglund, M., Becher, G. P., Schoning, K., Hansson, A., Nielsen, L., Clemmensen, L. B., Hede, M. U., Kroon, A., Pejrup, M., Sander, L., Stattegger, K., Schwarzer, K., Lampe, R., Lampe, M., Uścinowicz, S., Bitinas, A., Grudzinska, I., Vassiljev, J., Nirgi, T., Kublitskiy, Y. & Subetto, D. 2021: A Holocene relative sea-level database for the Baltic Sea. *Quaternary Science Reviews 266*, 107071, https://doi.org/10.1016/j.quascirev.2021.107071.
Sander, L., Fruergaard, M., Koch, J., Johannessen, P. N. & Pejrup, M. 2015a: Sedimentary indications and absolute chronology of Holocene relative sea-level changes retrieved from coastal lagoon deposits on Samsø, Denmark. *Boreas 44*, 706–720.
Sander, L., Fruergaard, M. & Pejrup, M. 2015b: Coastal landforms and the Holocene evolution of the island of Samsø, Denmark. *Journal of Maps 12*, 276–286.
Sander, L., Hede, M. U., Fruergaard, M., Nielsen, L., Clemmensen, L. B., Kroon, A., Johannessen, P. N., Nielsen, L. H. & Pejrup, M. 2016: Coastal lagoons and beach ridges as complementary sedimentary archives for the reconstruction of Holocene relative sea-level changes. *Terra Nova 28*, 43–49.
Sander, L., Michaelis, R., Papenmeier, S., Pravkin, S., Mollenhauer, G., Grotheer, H., Gentz, T. & Wiltshire, K. H. 2019: Indication of Holocene sea-level stability in the southern Laptev Sea recorded by beach ridges in north-east Siberia, Russia. *Polar Research 38*, 13. https://doi.org/10.33265/polar.v38.3379.
Strunk, A., Larsen, N. K., Nilsson, A., Seidenkrantz, M.-S., Levy, L. B., Olsen, J. & Lauridsen, T. L. 2018: Relative sea-level changes and ice sheet history in Finderup Land, North Greenland. *Frontiers in Earth Science 6*, 129, https://doi.org/10.3389/feart.2018.00129.
Sugisaki, S., Buylaert, J.-P., Murray, A., Tada, R., Zheng, H., Ke, W., Saito, K., Chao, L., Li, S. & Irino, T. 2015: OSL dating of fine-grained quartz from Holocene Yangtze delta sediments. *Quaternary Geochronology 30*, 226–232.
Tamura, T., Murakami, F., Nanayama, F., Watanabe, K. & Saito, Y. 2008: Groundpenetrating radar profiles of Holocene raised-beach deposits in the Kujukuri strand plain, Pacific coast of eastern Japan. *Marine Geology 248*, 11–27.
Tanner, W. F. 1993: An 8000-year record of sea-level change from grain-size parameters: data from beach ridges in Denmark. *The Holocene 3*, 220–231.
Van Heteren, S., Fitzgerald, D. M., Mckinlay, P. A. & Buynevich, I. V. 1998: Radar facies of paraglacial barrier systems: coastal New England, USA. *Sedimentology 45*, 181–200.
Vestøl, O., Ågren, J., Steffen, H., Kierulf, H. & Tarasov, L. 2019: NKG2016LU: a new land uplift model for Fennoscandia and the Baltic Region. *Journal of Geodesy 93*, 1759–1779.